Depth sensing and dissipation in tapping mode atomic force microscopy

Hugues Bodiguel, Hélène Montes, and Christian Fretigny[a)]
ESPCI, Laboratoire de Physico-Chimie des Polymères et des Matériaux Dispersés, CNRS UMR 7615, 10 rue Vauquelin, F-75231 Paris Cedex 05, France

(Received 29 December 2003; accepted 2 May 2004; published 26 July 2004)

Tapping mode atomic force microscopy is frequently used to image the surface of soft materials; it is also a powerful technique for nanomechanical analysis of surfaces. We report here an investigation of the depth sensing of the method on soft polymers. The chosen approach is based on the analysis of phase images of a model filled elastomer material. It leads to the determination of the depths of the hard particles lying under the surface. We found that tapping mode can probe interfaces buried under up to 80 nm of polymer. Under given tapping conditions, the penetration depth of the tip into the polymer is observed to depend on the layer thickness. However we show that, for a given penetration depth, the dissipated energy is independent of the thickness of the polymer layer under the tip. This suggests that the phase signal does not originate in the bulk viscoelasticity of the elastomer. Our observations support the hypothesis that, in tapping mode experiments on elastomers, the phase signal has an adhesive origin. Then, on surfaces with uniform interfacial properties, the phase images may reflect the local elastic properties of the sample, since they modify the tip-surface adhesive interactions. © *2004 American Institute of Physics.*
[DOI: 10.1063/1.1771495]

I. INTRODUCTION

During the past few years, atomic force microscopy (AFM) has become one of the most popular techniques for imaging the surface of many kinds of materials. One of the reasons that explain the success of this technique is certainly its ability to simultaneously image several properties of the surfaces (such as friction, adhesion, stiffness, etc.) in addition to the topography.[1,2] While a simple interpretation of the images in terms of topography, or on a qualitative basis is usually straightforward, a detailed interpretation of the contrasts is often difficult. This is particularly the case for mechanically soft samples, because the tip may induce deformation of the surface.[3,4] Thus, it is important to take into account the mechanics of the cantilever-tip-sample system.

Among the different AFM modes, tapping mode has proven to be particularly suitable for the analysis of soft samples. Much attention has been paid to phase angle measurements for their ability to give contrasts on heterogeneous materials. The description of the tapping mode has been the subject of many studies which revealed the nonlinear behavior of the oscillating cantilever.[1,2] A physical signification of the phase angle value was clearly suggested by Cleveland *et al.* a few years ago:[5] It is directly related to the dissipated energy per oscillation cycle. Nevertheless, the complexity of the tip-sample interaction leads to some difficulty in relating this dissipation to material properties. Indeed, viscoelasticity of the material as well as its adhesion properties may be involved in this dissipation.[6] More generally, while the principles of the technique appear to be understood,[1–7] their complexity calls for more experimental work in order to link the measured amplitudes or phase angles to surface or volume local properties.[8] A recent study[9] illustrated the phase angle dependence on volume properties in a tapping mode AFM experiment: It was found that volume heterogeneities may be observed under a gold layer up to 20 nm. One may expect this depth to be even higher for a soft surface.

A clear understanding of the possibilities of tapping mode AFM for nanomechanical studies would be of particular interest for thin polymer film analysis. Such films usually exhibit mechanical properties that may significantly differ from those of the bulk and have been the subject of many studies during the last decade.[10] These properties are found to depend both on the thickness of the film and on the properties of the substrate. During the last few years, several attempts have been made to investigate mechanical properties of thin films using different AFM techniques.[11] As for the other techniques used to analyze these systems, results are somewhat contradictory.

We use here a model nanocomposite material to experimentally study the response of tapping mode to materials mechanical properties. In a nanocomposite sample, made of rigid inclusions in a soft matrix, thin matrix layers separate the charges from the free surface. Thus, the surface of such a nanocomposite material offers the opportunity to study simultaneously thin films of different thicknesses. We present here a method for measuring the depths of rigid inclusions which can be observed in phase image of such a system. Then, we discuss the dissipation of the tip-surface interaction.

II. METHOD

To account for the contact mechanics on thin mechanically soft films deposited on a rigid substrate, one can define

a)Author to whom correspondence should be addressed; electronic mail: christian.fretigny@espci.fr

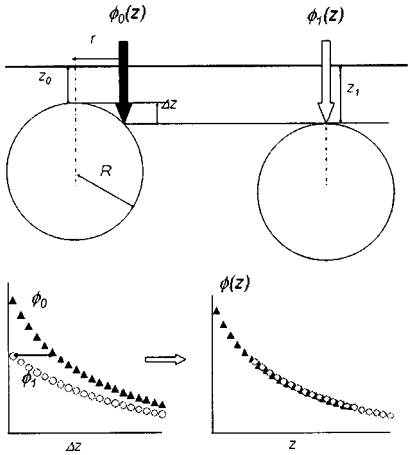

FIG. 1. Schematic representation of the filled elastomer (top). The measured phase ϕ is assumed to only depend on the layer thickness under the tip. Considering two particles lying at two different depths z_0 and z_1, the phase reaches the same values when the thicknesses are equal. This appends at a distance r of the center of the first particle, with $r^2=R^2-(R-(z_0-z_1))^2$. The relative depth $\Delta z=z_0-z_1$ can be determined. Schematic representation of the measured property as function of the depth increment for each particle (bottom left). One can displace the second curve to obtain a master curve (bottom right). The displacement value is the relative depth Δz of the two particles.

an apparent modulus for the layer and use classical contact mechanics on a semi-infinite medium.[12–15] This effective modulus is related to the confinement of the film between the indenter and the substrate and thus depends on the layer thickness. For hard inclusions in a soft matrix, we make the assumption that, under given experimental conditions, the phase angle ϕ, which is related to a local mechanical property, only depends on the local thickness of the polymer layer under the tip apex. This should indeed be the case if the phase angle is somewhat related to the apparent modulus of the confined layer between the tip and the surface of the inclusion. It should also hold as long as the tilt angle of the buried interface is not too large.

Let us consider a relatively soft material filled with identical spherical rigid particles of radius R. Assuming the surface to be fiat, the thickness $z(r)$ of the matrix layer at a distance r of the center of one particle is expressed as

$$z(r) = z_0 + \Delta z(r), \tag{1}$$

where z_0 is the depth of the buried particle interface, and

$$\Delta z(r) = R - \sqrt{R^2 - r^2} \tag{2}$$

is the depth increment corresponding to a radial displacement r.

As we assume the phase angle to depend only on the thickness, the phase image above a particle should present a radial symmetry. From its radial dependence $\phi(r)$ and according to the above expression, one can deduce the measured property as a function of the depth increment (Fig. 1). This depth increment can be considered as the local matrix thickness up to an unknown origin (z_0).

A large image containing n particles of various depths z_i leads to n different curves $\phi_i(\Delta z)$. A given depth may be probed by the tip at various radial positions of spheres situated at different depths. Then, assuming that the phase only depends on the local thickness z, the different curves $\phi_i(\Delta z)$ should be parts of a master curve $\phi(z)$ if their abscissa origin z_i was known (Fig. 1).

When enough particle depths are available in the image, it should be possible to construct the continuous curve $\phi(z)$ by displacing the n curves relative to each other. The corresponding displacements are the relative depths of the particles. The obtained master curve represents the variations of the phase ϕ versus the matrix layer thickness, up to an unknown origin. This origin can be determined if ϕ can be measured on a bare particle.

III. EXPERIMENT

The investigated sample is an elastomer composed of cross-linked polyethylacrylate chains reinforced with grafted silica nanoparticles. Reference 16 reports the synthesis and some characterizations of the silica particles and of the dispersion state of the filled elastomer. The particles are spherical with a mean radius of 45 nm and a small polydispersity (10%). These values were determined by both neutron and light scattering techniques and AFM measurements. Obtained data were in good agreement. The volume fraction of the nanoparticles in the studied sample is 10%(±1%) in volume, as determined by pyrolysis. Neutron scattering data reveal that the particles are well dispersed in the elastomer matrix.

The mechanical properties of both the cross-linked polyethylacrylate matrix and of the filled elastomer have been analyzed.[17] The glass transition temperature of the matrix, T_g, was found to be 244 K at 0.01 Hz. The loss modulus exhibits a maximum at $T=T_g$ with a magnitude of about 0.3 GPa.

All the experiments were conducted with a scanning probe microscope Multimode-Nanoscope III in tapping mode. We used a standard rectangular cantilever (Nanosensors NCL-W), with a resonance frequency of 166.704 kHz (quality factor $Q=451$) and a typical spring constant of about 40 N/m. Phase angle measurement was performed by a lock-in amplifier (7280 DSP EG&G Instruments). Special care has been taken in mounting the cantilever in the microscope in order to get a clean resonance shape. The phase reference was chosen in order that the measured phase angle is zero at frequencies much lower than the resonance one. The excitation phase was −65°. All the images were acquired on the same area at 1 Hz, over 1×1 μm^2 with a resolution of 512×512 pixels.

IV. RESULTS AND DISCUSSION

A. Data analysis

First, it is verified that the sample surface is sufficiently fiat to allow the analysis presented above. On soft materials, tapping mode height measurements frequently mix topographical and mechanical properties of the surface.[18] It is however expected that under soft tapping conditions, the deformation of the surface induced by the tip is relatively small and thus is expected to play a minor role in the imagery process.[4,19] We thus used soft tapping conditions to obtain a topographic image of the sample. Figure 2 presents the

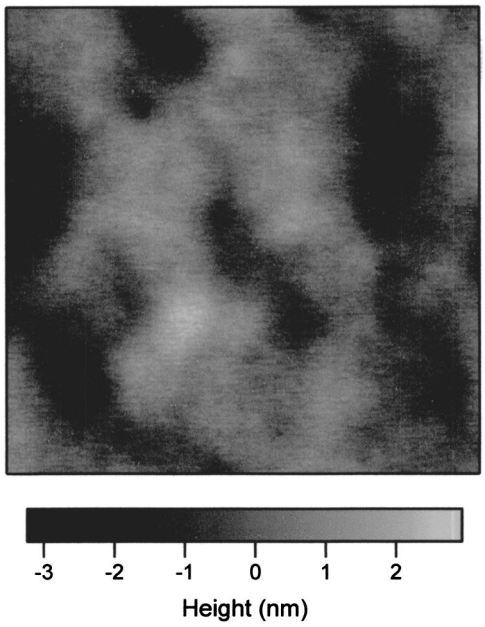

FIG. 2. 1 μm$\times$1 μm height image of the reinforced polyethylacrylate sample. The image was obtained with a low amplitude (A_0=25 nm) and a high set-point ratio (A/A_0=0.9). The roughness is about 0.9 nm.

height image obtained in repulsive mode, under a low excitation amplitude (free amplitude A_0=25 nm) and rather high set-point ratio (A/A_0=0.9, with A the oscillation amplitude). No emerging particles can be seen and roughness is about 0.9 nm over a scanned area of 1 μm^2. This is an indication that the particles lie under a flat polymer layer.

One of the phase image used for the analysis is presented in Fig. 3 (A_0=134 nm, A/A_0=0.7). Under these conditions,

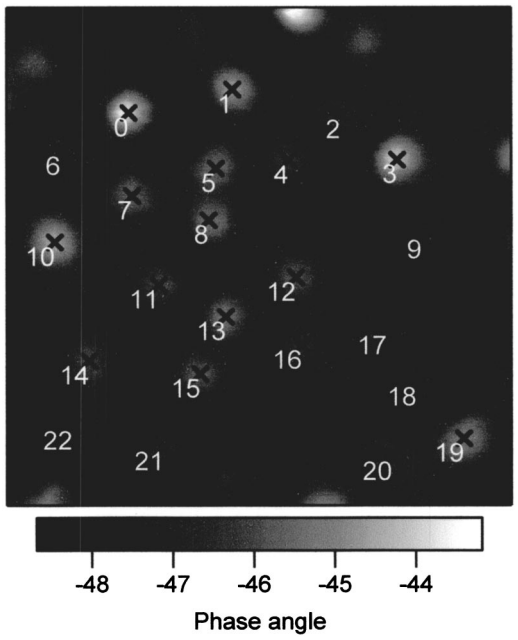

FIG. 3. 1 μm$\times$1 μm phase image of the reinforced polyethylacrylate sample (same area as Fig. 2). The image was obtained with a high amplitude (A_0=134 nm) and a low set-point ration (A/A_0=0.7). The added black crosses correspond to maxima positions of the phase angle, determined by a local parabolic fit. Each maximum position is labeled with an arbitrary number.

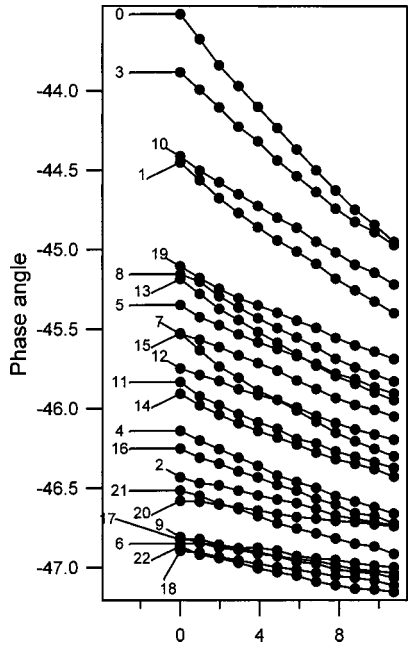

FIG. 4. Computed phase angle averages as function of the depth increment Δz calculated from the mean radius R=45 nm of the silica nanoparticles: $\Delta z = R - \sqrt{R^2 - r^2}$, with r the distance from the corresponding phase maximum position. The phase angle average is calculated on annuli of increasing radius set according to Eq. (3), with a constant area of 72 pixels (275 nm^2). They were obtained on four images with the same tapping condition, including the one shown in Fig. 3, and then averaged. Each trace is labeled with the number attributed to the corresponding maximum in Fig. 3.

the phase angle contrast is relatively high. The positions of the maxima of the phase signal are likely to be at the top of the silica nanoparticles. 23 particles detected in the imaged region were labeled (0–22) and used for the analysis. The positions of their center are precisely determined by a local paraboloidal fit on portions of the image which contain each maximum. From these positions, the phase angle decreases with the radial distance, as the thickness of the polymer layer increases. The radial variation of the signal is computed for each particle through an angular average of the phase on annuli of increasing mean radius, centered on the top of the particles. In order to obtain equally weighted experimental points, the average is calculated on a constant number of pixels. To achieve this, the inner and outer radii of the annulus, r_i and r_i+1, respectively, were set according to the following expression:

$$r_i^2 = \frac{Na^2}{2\pi} i, \tag{3}$$

where N is the number of pixels used for the average calculation, and a the size of a pixel. For the analysis presented here, we used N=80 and a=1.95 nm. The phase angle data as a function of the depth increment for each particle was determined on four images of the same region of the sample, with the same tapping conditions and are then averaged. The result is presented in Fig. 4. The standard deviations of the phase angle is approximately 2% of the mean value, leading to error bars shorter than the dots sizes of Fig. 4. In order to keep a small value for the tilt angle of the buried interface, the range of depth increment analyzed for each sphere is

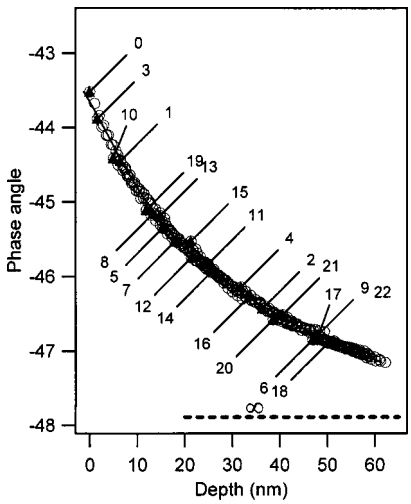

FIG. 5. Master curve obtained after the horizontal displacements z_i of the curves of Fig. 3 (circles). The start of each trace is represented (black triangle) and labeled with the corresponding number. The displacements are computed via a polynomial fit of degree 5 (solid line). The phase angle on the polymeric matrix is shown and labeled ∞. It should represent the asymptotic behavior of the master curve for an infinite depth. The depth of the zero-labeled particle is arbitrary set to zero.

limited to 9 nm, which correspond to a maximal tilt angle for the tangent plane to the sphere of 40°. The data labeled ∞ are obtained above a region apparently free of particles near the surface and would correspond to the response of a semi-infinite polymer layer.

The last part of the analysis consists in the determination of the master curve representing the phase angle as a function of depth. The experimental curves corresponding to each of the particles are displaced in order to form a continuous master curve. For this purpose, we used a least squared fit of the displaced experimental data with a polynomial function. The determined parameters are the depths relative to one reference particle (#0) and the polynomial coefficients. The displacement results are not sensitive to the degree of the polynomial used, between degree 3 and 13. The master curve

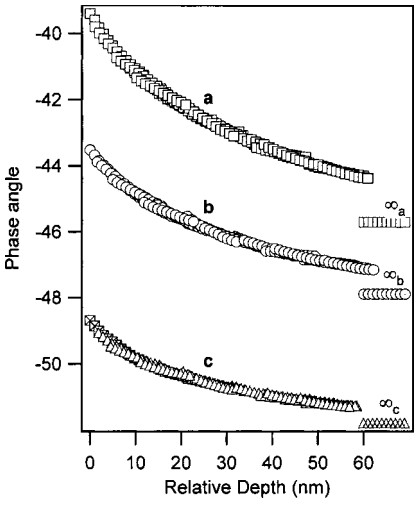

FIG. 6. Master curves for the depth dependence of the phase for three tapping conditions: $A/A_0=0.6$ (a), 0.7 (b), and 0.8 (c). The phase angle values on the polymeric matrix are also shown and are, respectively, labeled ∞_a, ∞_b, and ∞_c.

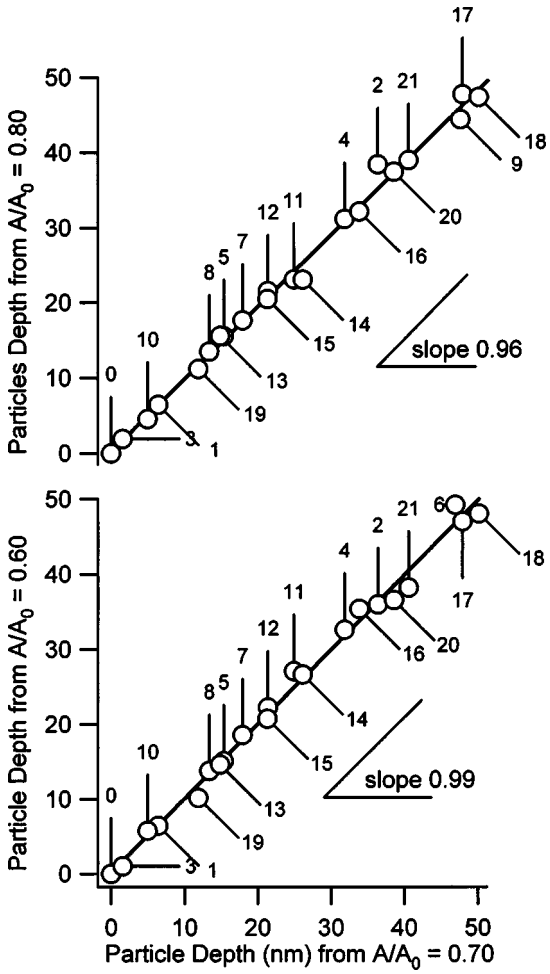

FIG. 7. Correlations of the determined relative depth of the silica nanoparticle (circles) between the three experimental conditions used. (a) Particle depths determined from the $A/A_0=0.6$ image versus the ones from $A/A_0=0.7$ (b) Particle depths determined from the $A/A_0=0.8$ image versus the ones from $A/A_0=0.7$. The linear fits (solid lines) slopes are, respectively, 0.99 and 0.96 (±0.02).

presented in Fig. 5 is obtained with a polynomial function of the fifth degree. It appears to be continuous, justifying *a posteriori* its existence, and the assumptions we made. As mentioned above, these calculated depths are relative to a reference which is set here to be the depth of the closest particle to the free surface.

We apply the method on the same region of the sample, with two other tapping conditions: Identical free amplitude but different set-point ratios ($A/A_0=0.6$ and 0.8). Figure 6 presents the obtained results for the three tapping conditions.

As a check for the consistency of the method, it is important to verify that the determined depths are independent of the experimental conditions used to record the images. Figure 7 shows the correlation of the calculated depth of each of the silica particles between the different conditions: Particle depths determined with the two extreme conditions are plotted versus the ones determined with the intermediate condition detailed above. We found a linear correlation with a slope very close to unity, showing that, in the tested range, the calculated depths do not depend on the experimental conditions. These good correlations between the different tap-

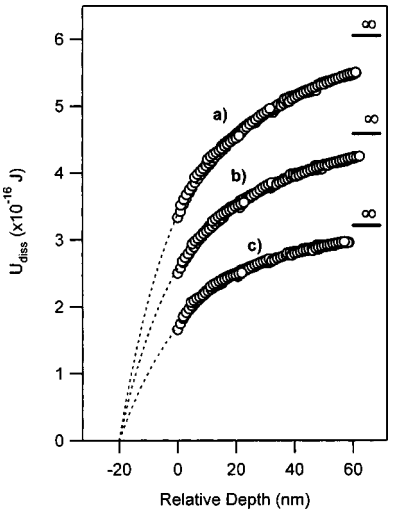

FIG. 8. Master curves of the dissipated energy versus the relative depths, deduced from the master curves obtained at three different set-point ratios: 0.6 (a), 0.7 (b), 0.8 (c). The dissipated energy is deduced from the phase angle master curves according to Eq. (4). The extrapolations to zero (dashed curves) are guides for the eyes. They give an idea of the zero depth.

ping conditions validate the method and the assumptions made.

B. Absolute particle depths

In principle, to get an absolute reference for the particles depths, it would have been necessary to analyze data taken on a few particles nearly tangent to the free surface of the sample. As the studied sample did not exhibit such features, a direct determination is not possible. A discussion is presented below to estimate such a reference.

For given tapping conditions, phase angle on silica could be considered as the value that would have been obtained for a vanishing layer thickness. Extrapolation of the master curve representing the phase angle as a function of the relative depth until this phase value would set the reference depth. It is however not possible to use the previous tapping conditions on a hard surface, because this would have broken the tip.

Rather than an extrapolation of the phase angle measured at a low amplitude reduction, it seems convenient to discuss the dissipated energy in the tip-surface interaction. Phase angle is simply related to the dissipated energy per oscillation U_{diss}.[5] It can be expressed as

$$U_{\mathrm{diss}} = \frac{\pi k A A_0}{Q}\left(\frac{\sin\phi}{\sin\phi_0} - \frac{A}{A_0}\right), \tag{4}$$

where A_0 and ϕ_0 are the amplitude and the phase angle when the tip is far from the surface, Q is the quality factor, and k is the cantilever spring constant. These parameters are experimentally determined, except for the spring constant for which we used the constructor's value.

As the thickness of the polymer layer vanishes, we expect the dissipated energy to become negligible as compared to that which can be measured on a soft sample. Indeed, it is shown below that the high dissipation measured on polymer layers mainly originates in their high adhesion properties, related to the softness of the material, which gives rise to large contact areas.

Figure 8 shows the master curves representing the dissipated energy as functions of the relative depths, for the three tested tapping conditions. The gap between zero and the lowest experimental value (the one on the top of the particle which is the closest to surface) is quite high when compared to the order of the measured range of energy. This makes the determination of the depth reference rather difficult. However, by keeping constant the curvature of these three curves, we found that the dissipated energy vanishes at a relative depth of about 20 nm. The extrapolations in Fig. 8 are pure attempts and should only be considered as a guide for the eyes. Different extrapolation could have been made, but they would have lead to similar order of magnitude for the depth reference, i.e., between 10 and 30 nm. Then it can be concluded that on the studied polymer, buried rigid interface as deep as 80 nm can be probed by phase imaging. Assuming, as it is usually made in contact mechanics[20] that the domain which participates to the mechanical response of a contact has a size which represents about 10 times the contact size, the obtained values would correspond to contact size of less than about 10 nm at most. Such an estimation appears to be consistent with the analysis of the indentation which is presented in the next section.

C. Influence of the particle geometry

The particles used in this study exhibit a relatively small polydispersity of 0.1. A small variation of the particle radius slightly modifies the slopes of the curves $\phi(\Delta z)$ displayed in Fig. 4. With several particles in a narrow range of depth, these variations are averaged, and thus do not lead to significant errors concerning the determination of the master curve.

On the contrary, an error on the mean radius would lead to a global modification of the depth range. The particle radius was determined by several methods that were in good agreement. A maximum error of 2 nm for the mean radius can be estimated. On another hand, the existence of a glassy shell around the particles[17] may lead to a higher apparent radius for the particles. The thickness of this shell is about 2 nm, which is small as compared to the particle radius. It would lead to a relative deviation of the determined depths of about 5%. We thus conclude that the polydispersity of the particles and small errors on the mean radius do not lead to significant errors on the calculated particle depths.

V. INDENTATION-DISSIPATION

From Fig. 6, it appears that the more the amplitude is reduced as compared to the free amplitude, the larger the phase contrast depends on the polymer film thickness. Thus, hardening the tapping conditions enhances the phase angle contrast on volume properties. It was often pointed out[4,19] that the volume contributions of the tip-sample interaction depends on the experimental conditions. Soft tapping conditions correspond to a low free amplitude with a set-point ratio close to unity and hard tapping for a high free amplitude and a smaller set-point ratio (0.5–0.8). Moderate or

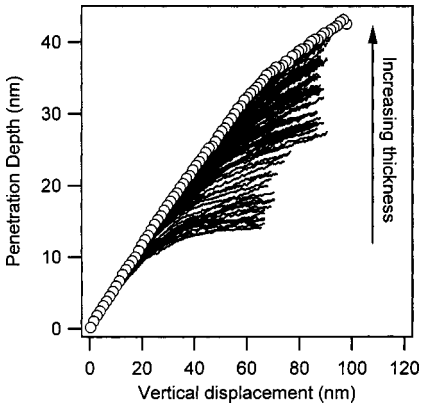

FIG. 9. Penetration depths versus the vertical displacement. The data are deduced from amplitude approach–retract curves by computing the difference between the measured amplitude and the extrapolated amplitude obtained on a hard surface. The approach–retract curves were obtained at different positions on the sample: above and around the top of three particles (lines) and on the semi-infinite polymer matrix (circles). The lower the layer thickness under the tip, the lower the penetration.

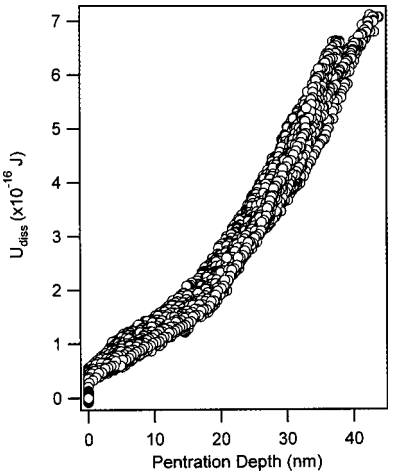

FIG. 10. Dissipated energy as a function of the penetration depth. The penetration depths are those reported in Fig. 9, the dissipated energy was calculated from the phase and amplitude approach–retract curves, according to Eq. (4). All the curves seem to define a master curve.

hard tapping is sensitive to a volume below the surface, whereas soft tapping is believed to probe mainly surface properties. The results presented above constitute an experimental basis to discuss this effect.

Phase angle is essentially the dissipated energy per oscillation cycle [see Eq. (4)]. Figure 7 shows that this dissipation is strongly dependent on the layer thickness. In this section, we examine this contrast, by the means of approach–retract experiments. The distance between the equilibrium position of the cantilever and the surface is periodically modulated, above fixed points of the sample. The oscillation amplitude and phase are simultaneously recorded.

Approach–retract experiments were performed at different locations of the region of the sample used for the previous analysis. Data taken on top of and around three spheres are gathered together with data on a region where no spheres are observed. We determined the tip penetration depth by computing the difference between the measured amplitude in an approach–retract experiment with the one on silicon.[4,21] Results are presented in Fig. 9. The penetration seems to saturate above the thinner layers (lower curves), while for thicker layers, this effect takes place later. A similar behavior has been found on block copolymers by Knoll *et al.*:[4] Above rigid blocks, the indentation levels off at a lower value than on soft regions. Here, indentations of a few tens of nanometers are consistent with the observed range of depths of the silica balls discussed above. The high sensitivity of the penetration depth to the polymer thickness may be understood as follows: the repulsive force acting on the cantilever increases when the layer thickness decreases. This is consistent with the increase of the apparent modulus for a confined medium.[13–15] The large differences of the indentation depths on the studied sample are associated with important contrasts in the corresponding height images. Indeed, while almost no contrast is present while gentle tapping conditions are used (see Fig. 2), large contrasts exist on height images under harder tapping conditions (not shown). This is an example of mechanical effects in height images.[4,18] From the present data, the contact radius is rather difficultly estimated since it would require a precise description of the tip end shape. Nevertheless, a rough estimate, using a paraboloid shape of curvature radius of 5 nm, leads to a contact size of about 15 nm at most when no sphere is present. This value is consistent with the observed depth range, discussed in the preceding section.

The dissipated energy dependence on the penetration depth is shown in Fig. 10. As seen on this plot, all the traces seem to form a master curve. This indicates that the dissipated energy only depends on the penetration depth and does not vary much with the layer thickness. Thus, although the apparent modulus increases when reducing the thickness, this is not the case for the dissipation. The variation of the dissipated energy with the layer thickness as seen in Fig. 8 is thus only due to the high sensitivity of the penetration depth to the apparent modulus under the tip.

One may think of two different origins for the dissipation in a tapping mode experiment on a viscoelastic material.[6] The first one is the bulk viscoelastic dissipation, which can be relevant for high penetration depths.[22] The second possible origin is related to adhesion. At a given penetration depth, bulk viscoelastic dissipation should depend on the layer thickness, since the local effective loss modulus depends on this parameter. On the contrary, the independence of the dissipated energy on the layer thickness at a given penetration depth is a clear indication that adhesion contribution dominates the dissipation. Indeed, in a tapping experiment, the range of contact times is short enough that the adhesive equilibrium for the contact is certainly not reached. While indenting the material, one may consider that the adhesion forces have no effect on the growing of the contact area. The contact may be considered as mainly Hertzian. During the tip ejection, on the contrary, the contact area must diminish, involving adhesive dissipation. Dissipation is controlled by the penetration depth at the end of the indentation phase. Then, at a given penetration depth, the adhesive dissipation energy is not dependent on the bulk material properties (effective modulus) as observed in Fig. 10. Such a model has been successfully used to describe the rebound of

a rigid ball on a rubber surface.[23] The detailed analysis of the mechanical behavior of thin polymer films using this description is beyond the scope of this article and constitute a part of our future work.

VI. DISCUSSION

This paper introduces a method for determining the thickness dependence of tapping mode phase signal. One direct application is the determination of the depths where lie the particles of a nanocomposite material, observed in an AFM image. We found that phase is sensitive to hard particles lying up to 80 nm under the surface. Thus, using relatively hard tapping conditions on soft materials, the phase angle is sensitive to deep volume properties. The studied sample surface allows to easily study several thicknesses of polymer films in avoiding the preparation of different samples. The knowledge of the depths of hard inclusions may constitute a first step for the study of size-dependent mechanical properties, such as the apparent modulus or dissipation properties. In this article, we focused on the energy dissipated during the tip-sample intermittent contact. This energy was found to be independent of the thickness of the polymer layer for a given tip penetration depth. These observations are indications that the dissipated energy, measured during a tapping mode experiment through the phase angle, does not have a bulk viscoelastic origin on the elastomer matrix, even at large penetration depths. We propose that they are related to the rupture of the adhesive contact during the tip ejection. Such a conclusion has been drawn by analyzing rather hard tapping conditions; it should *a fortiori* apply for gentler ones. Using time-temperature superposition principle,[24] the glass transition temperature of the polymer matrix can be roughly estimated to be just below room temperature at the tapping frequency.[25] Then, even under such highly dissipative conditions, the phase signal appears to be controlled by adhesion. It can be concluded that this should generally apply for most elastomer samples.

The use of geometrically well-defined inclusions to test the depth sensitivity of tapping mode phase signal and dissipation mechanisms can be extended to other locally measured properties. Friction, for instance, is known to originate from bulk and interfacial properties.[26] It should be possible to discuss friction mechanisms using experiments similar to the ones presented here.

[1] R. Garcia and R. Pérez, Surf. Sci. **47**, 197 (2002).
[2] F. J. Gessibl, Rev. Mod. Phys. **75**, 949 (2003).
[3] J. Tamayo and R. Garcia, Langmuir **12**, 4430 (1996).
[4] A. Knoll, R. Magerle, and G. Krausch, Macromolecules **34**, 4159 (2001).
[5] J. P. Cleveland, B. Anczykowski, A. E. Schmid, and V. B. Elings, Appl. Phys. Lett. **72**, 2613 (1998).
[6] R. Garcia, J. Tamayo, M. Calleja, and F. Garcia, Appl. Phys. A: Mater. Sci. Process. **A66**, S309 (1998).
[7] L. Nony, R. Boisgard, and J.-P. Aimé, J. Chem. Phys. **111**, 1 (1999).
[8] O. P. Behrend, L. Odoni, J. L. Loubet, and N. A. Burnham, Appl. Phys. Lett. **75**, 2551 (1999).
[9] A. Berquand, P.-E. Mazeran, and J.-M. Laval, Surf. Sci. **523**, 125 (2003).
[10] See, for example, J. L. Keddie, R. A. L. Jones, and R. A. Gory, Europhys. Lett. **27**, 59 (1994); J. A. Forrest and K. Dalnoki-Veress, Adv. Colloid Interface Sci. **94**, 167 (2001); D. Long and F. Lequeux, Eur. Phys. J. E **4**, 371 (2001).
[11] See, for example, D. Johannsmann, Eur. Phys. J. E **8**, 257 (2002); S. Ge, Y. Pu, W. Zhang, M. Rafailovich, J. Sokolov, C. Buenviaje, R. Buckmaster, and R. M. Overney, Phys. Rev. Lett. **85**, 2340 (2000); X. P. Wang X. Xiao, and O. K. C. Tsui, Macromolecules **34**, 4180 (2001).
[12] M. F. Doerner and W. D. Nix, J. Mater. Res. **1**, 601 (1986).
[13] H. Gao, C.-H. Chiu, and J. Lee, Int. J. Solids Struct. **29**, 2471 (1992).
[14] J. Mencik, D. Munz, E. Quandt, and E. R. Weppelmann, J. Mater. Res. **12**, 2475 (1997).
[15] A. Perriot and E. Barthel J. Mater. Res. **19**, 600 (2004).
[16] J. Berriot, H. Montes, F. Martin, W. Pyckhout-Hintzen, G. Meier, and H. Frielinghaus, Polymer **44**, 4909 (2003).
[17] J. Berriot, H. Montes, F. Lequeux, D. Long, and P. Sotta, Macromolecules **35**, 9756 (2002).
[18] S. Kopp-Marsaudon, P. Leclère, F. Dubourg, R. Lazzaroni, and J.-P. Aimé, Langmuir **16**, 8432 (2000).
[19] S. N. Magonov, V. Ellings, and M. H. Whangbo, Surf. Sci. Lett. **375**, L385 (1997).
[20] K. L. Johnson, *Contact Mechanics* (Cambridge University Press, Cambridge, UK, 1994).
[21] F. Dubourg, S. Kopp-Marsaudon, P. Leclère, R. Lazzaroni, and J.-P. Aimé, Eur. Phys. J. E **6**, 387 (2001).
[22] B. Bhushan and J. Qi, Nanotechnology **14**, 886 (2003).
[23] M. Barquins and J.-C. Charmet, C. R. Acad. Sci., Ser. IIa: Sci. Terre Planetes **318**, 721 (1994).
[24] J. D. Ferry, *Viscoelastic Properties of Polymers*, 2nd ed. (Wiley, New York, 1970).
[25] J. Berriot, Ph.D thesis, Université Paris 6, 2003.
[26] D. Tabor, in *Fundamentals of Friction: Macroscopic and Microscopic Processes*, edited by I. Singer and H. Pollock, NATO ASI Series (Kluwer Academic, Dordrecht, Boston, London, 1992), Vol. 220.